

INORGANIC CHEMISTRY

Terminal coordination of diatomic boron monofluoride to iron

Myles J. Drance¹, Jeffrey D. Sears², Anthony M. Mrse¹, Curtis E. Moore¹, Arnold L. Rheingold¹, Michael L. Neidig², Joshua S. Figueroa^{1*}

Boron monofluoride (BF) is a diatomic molecule with 10 valence electrons, isoelectronic to carbon monoxide (CO). Unlike CO, which is a stable molecule at room temperature and readily serves as both a bridging and terminal ligand to transition metals, BF is unstable below 1800°C in the gas phase, and its coordination chemistry is substantially limited. Here, we report the isolation of the iron complex $\text{Fe}(\text{BF})(\text{CO})_2(\text{CNAr}^{\text{Tripp2}})_2$ [$\text{Ar}^{\text{Tripp2}}$, 2,6-(2,4,6-(*i*-Pr)₃C₆H₂)₂C₆H₃; *i*-Pr, *iso*-propyl], featuring a terminal BF ligand. Single-crystal x-ray diffraction as well as nuclear magnetic resonance, infrared, and Mössbauer spectroscopic studies on $\text{Fe}(\text{BF})(\text{CO})_2(\text{CNAr}^{\text{Tripp2}})_2$ and the isoelectronic dinitrogen (N₂) and CO complexes $\text{Fe}(\text{N}_2)(\text{CO})_2(\text{CNAr}^{\text{Tripp2}})_2$ and $\text{Fe}(\text{CO})_3(\text{CNAr}^{\text{Tripp2}})_2$ demonstrate that the terminal BF ligand possesses particularly strong σ -donor and π -acceptor properties. Density functional theory and electron-density topology calculations support this conclusion.

Carbon monoxide (CO) is among the most widely studied ligands in organometallic chemistry. Since the original report of a CO coordination compound 150 years ago (1) and the discovery of the first homoleptic metal carbonyl $\text{Ni}(\text{CO})_4$ in 1890 (2), the coordination chemistry of CO has occupied a central role in the development of the reactivity and electronic structure theory of transition-metal complexes (3, 4). The binding of CO to transition metals has been described classically by the Dewar-Chatt-Duncanson bonding model (5, 6). In the terminal coordination mode, σ -donation from the carbon-centered lone pair of CO to an empty, acceptor orbital on the metal provides a primary bonding interaction (Fig. 1A). However, this metal-CO linkage is fortified by π -backdonation interactions from filled metal-based d-orbitals to the π^* orbitals of CO (Fig. 1A) (7). The success of CO as a ligand is derived from the polarized nature of the C–O triple bond, which renders both its σ -donor and π -acceptor functionalities energetically well matched for interaction with a transition metal (8). Diatomic molecules and ions that are isoelectronic and isolobal to CO—such as N₂, CN[−], and NO⁺ (Fig. 1B)—are also widely known to bind transition metals (9). However, the less polarized nature of these diatomics substantially alters their properties as ligands. Indeed, N₂ has comparatively lower-energy σ -donor orbitals and higher-energy π^* orbitals than those of CO, which limits its binding ability (8, 9). In addition, the π^* orbitals of CN[−] are too high in energy for effective π -backdonation, and although NO⁺ is a strong π -acid, it is a relatively weak σ -donor ligand (8, 9).

It has long been recognized that the quintessential neutral, yet highly polarized, isoelectronic

analog to CO is boron monofluoride (BF) (Fig. 1C) (10–15). Diatomic BF has been predicted to bind even more favorably to transition metals owing to a decreased HOMO/LUMO gap (HOMO, highest occupied molecular orbital; LUMO, lowest unoccupied molecular orbital) relative to that of CO, leading to both more potent σ -donor and π -acceptor abilities (16–19). However, this electronic feature also renders the free BF molecule far more reactive than CO. As such, BF is not a stable molecule at room temperature. It must be prepared under low pressure at 1800° to 2000°C, and it quickly oligomerizes upon cooling (11, 12, 14). Whereas coordination to transition metals is often used as a strategy for the stabilization of highly reactive species, fluoroborylene complexes, in which BF serves as a terminal ligand, have remained long-sought synthetic targets that have eluded isolation (14, 20–24). Here, we report the preparation and x-ray crystal structure of a terminal fluoroborylene complex of iron that possesses sufficient kinetic stability for isolation at room temperature. In addition, the iron-based molecular platform presented here allows for the direct comparison of the structural and electronic consequences of BF coordination relative to those of the neutral isoelectronic diatomic molecules CO and N₂.

To prepare a terminal fluoroborylene complex amenable to isolation, we chose to construct the BF unit directly within the coordination sphere of a kinetically stabilizing metal center. Previously, Vidovic and Aldridge reported that two equivalents of the ruthenium-based nucleophile $\text{Na}[\text{CpRu}(\text{CO})_2]$ (Cp, cyclopentadienyl; $[\text{C}_5\text{H}_5]^-$) reacts with boron trifluoride diethyl etherate (BF₃·Et₂O) with the formal loss of two equivalents of sodium fluoride (NaF) to produce the bridging BF complex $(\mu_2\text{-BF})[\text{CpRu}(\text{CO})_2]_2$ (20). The latter is the only crystallographically characterized compound in which BF functions as a ligand to a metal center. We reasoned that a mononuclear terminal BF complex could be

similarly obtained through salt elimination, if a sterically encumbered, dianionic metal-based nucleophile were used to prevent the addition of two metals to a single boron atom. Accordingly, the formally Fe(II) species, $\text{K}_2[\text{Fe}(\text{CO})_2(\text{CNAr}^{\text{Tripp2}})_2]$ ($\text{K}_2[\mathbf{1}]$; $\text{Ar}^{\text{Tripp2}}$, 2,6-(2,4,6-(*i*-Pr)₃C₆H₂)₂C₆H₃; *i*-Pr, *iso*-propyl) (Fig. 1D), was deemed suitable for this purpose because of the presence of two encumbering *meta*-terphenyl isocyanide ligands (25) and its overall isolobal relationship to the well-known dianionic, iron-based nucleophile $[\text{Fe}(\text{CO})_4]^{2-}$ (26).

Treatment of $\text{K}_2[\mathbf{1}]$ with 1.0 equivalent of BF₃·Et₂O in a cold diethyl ether/*n*-hexane mixture (9:1; −100°C), followed by the removal of salts and analysis by ¹H nuclear magnetic resonance (NMR) spectroscopy, revealed the presence of unreacted $\text{K}_2[\mathbf{1}]$ and a new diamagnetic product in a 1:1 ratio. However, treatment of $\text{K}_2[\mathbf{1}]$ with 2.0 equivalents of BF₃·Et₂O under the same conditions resulted in a distinct color change to yellow-brown from red, with ¹H NMR spectroscopy indicating ~90% conversion to this new product (Fig. 1D). Crystallization of the reaction mixture from *n*-hexane produced yellow single crystals, which were determined by means of x-ray crystallography to be the five-coordinate complex $\text{Fe}(\text{BF})(\text{CO})_2(\text{CNAr}^{\text{Tripp2}})_2$ (**2**), featuring a terminally bound fluoroborylene ligand (Fig. 2A). Analysis by means of ¹⁹F NMR spectroscopy of the salts produced from the reaction revealed tetrafluoroborate ($[\text{BF}_4]^-$) ion as a by-product (figs. S11 and S12), suggesting that a second equivalent of BF₃ promotes fluoride loss during the formation of **2**. A reasonable mechanism for the formation of **2** is one that proceeds through an unobserved iron difluoroboryl intermediate (Fig. 1D, **Int**), the formation or fragmentation of which through fluoride ion elimination is aided by a second equivalent of BF₃. Accordingly, this inference allowed the synthesis to be optimized by using 2.8 equivalents of BF₃·Et₂O (Fig. 1D), which resulted in the complete conversion to **2** and allowed for its isolation as a room-temperature stable, yellow crystalline material in 82% yield.

Complex **2** is an isolobal analog to the simple, yet hypothetical, molecular species $\text{Fe}(\text{BF})(\text{CO})_4$, which is the most well-considered theoretical and computational model of a fluoroborylene complex (16–19). In line with this analogy, the axial $\angle \text{C1-Fe-C2}$ bond angle in **2** [160.38(7)°; numbers in parentheses indicate estimated standard deviation] is in excellent agreement with the $\angle \text{C}_{\text{ax}}\text{-Fe-C}_{\text{ax}}$ (163.4°; ax, axial) bond angle previously predicted for $\text{Fe}(\text{BF})(\text{CO})_4$, as are the equatorial $\text{C}_{\text{eq}}\text{-Fe-B}$ angles [124.6° (average) for **2** versus 123.4° for $\text{Fe}(\text{BF})(\text{CO})_4$; eq, equatorial] (17, 19). This pronounced distortion from an ideal trigonal bipyramidal geometry results from the strong σ -donor properties of the BF ligand, which, owing to orbital mixing in *C*_{2v} symmetry, imparts substantial antibonding character on an otherwise nonbonding orbital directed toward the axial isocyanide ligands (17, 19). In addition, the Fe–B bond distance in **2** [1.7703(25) Å] is the shortest reported for a transition metal–boron bond

¹Department of Chemistry and Biochemistry, University of California, San Diego, 9500 Gilman Drive, Mail Code 0358, La Jolla, CA 92093-0358, USA. ²Department of Chemistry, University of Rochester, Rochester, NY 14627, USA.

*Corresponding author. Email: jsfig@ucsd.edu

(fig. S28). Accordingly, this metrical parameter reflects substantial π -interactions between the BF unit and the iron center, which are in accord with the ligand's predicted strong π -acceptor properties (17). However, the B–F bond distance in **2** [1.2769(29) Å] is the shortest known for any structurally characterized boron-fluorine compound (figs. S29 and S30) and compares well with the equilibrium internuclear separation of free BF in the gas phase [1.262672(7) Å] (14).

The diamagnetism of **2** allows for an assessment of the BF unit with NMR spectroscopy. In benzene- d_6 solution, **2** gives rise to a broad ^{11}B NMR signal centered at $\delta_{\text{B}} = +56.5$ parts per million (ppm) (full width at half maximum = 1820 Hz). This chemical shift is most similar to those of transition-metal aminoborylene complexes ($\text{M}, \text{B}-\text{NR}_2$; $\delta_{\text{B}} = +60$ to 90 ppm) (27) and is downfield of that for the formally platinum(II) oxyboryl complex *trans*-Pt(BO)Br(PCy₃)₂ ($\delta_{\text{B}} = +17$ ppm) that features a B–O triple bond akin to the cyanide ion ([CN][−]) (28). This difference

in chemical shift signifies that π -donation from fluorine to boron in **2** is substantially diminished relative to B–O π -bonding in the oxyboryl group and is reflective of the greater electronegativity of the fluorine atom in the BF unit. Complex **2** also gives rise to a ^{19}F NMR resonance at $\delta_{\text{F}} = +1.6$ ppm, which is significantly downfield relative to that found in the dinuclear bridging BF complex (μ_2 -BF)[CpRu(CO)₂]₂ ($\delta_{\text{F}} = -185.0$ ppm) (20) and BF₃·Et₂O ($\delta_{\text{F}} = -153$ ppm). Rapid quadrupolar relaxation of the $I = 3/2$ ^{11}B nucleus prevented a determination of the $^1J_{\text{BF}}$ coupling constant in both the one-dimensional (1D) ^{11}B and ^{19}F NMR spectra of **2**. However, 2D ^{19}F – ^{11}B heteronuclear multiple-quantum coherence NMR experiments (fig. S10) (29, 30) showed maximum cross-peak signal intensity in the measurement optimized for $^1J_{\text{BF}} = 650$ Hz. This extremely large implied coupling constant is consistent with the very short B–F bond distance observed in the x-ray structure of complex **2**. It also indicates that a high degree of boron s-orbital character

is a major component of the bonding within the B–F ligand.

To further evaluate the structural and electronic effects of terminal BF coordination, the isoelectronic dinitrogen and CO complexes Fe(N₂)(CO)₂(CNAr^{Tripp2})₂ (**3**) and Fe(CO)₃(CNAr^{Tripp2})₂ (**4**) were prepared and characterized by means of x-ray crystallography (Fig. 2A). Complexes **3** and **4** both adopt undistorted trigonal bipyramidal coordination geometries, as indicated by near-linear axial isocyanide $\angle \text{C1}–\text{Fe}–\text{C2}$ angles [179.05(14)° for **3**; 178.61(22)° for **4**]. These metrical parameters contrast with the significantly bent $\angle \text{C1}–\text{Fe}–\text{C2}$ angle of complex **2** and support the notion that both CO and N₂ are weaker σ -donors than the BF ligand (17). Similarly, the infrared (IR) spectroscopic data of the complexes show a clear redshift of the asymmetric ν_{CN} stretch in the order **4** > **3** > **2** (Fig. 2A), further illustrating that the σ -donor ability of BF is greatest relative to CO and N₂. Accordingly, when coupled with the short Fe–B bond length in **2**, the structural and spectroscopic comparison provided by complexes **3** and **4** offers complementary support to the conclusion that BF possesses simultaneously strong σ -donor and π -acceptor characteristics. This distinct electronic character of the BF ligand is further confirmed by the Mössbauer spectroscopic data of **2**, **3**, and **4** (figs. S13 to S15). Of the series, complex **2** gives rise to the most negative isomer shift ($\delta = -0.15$ mms^{−1}), followed by **4** then **3** ($\delta = -0.08$ and $+0.08$ mms^{−1}, respectively). This trend indicates that the total bonding interactions (31) to the iron center are greatest for complex **2** and diminish predictably as both the σ -donor and π -acceptor abilities of CO and N₂ weaken. Furthermore, the Mössbauer quadrupolar-splitting values (ΔE_{Q}), which are sensitive to the iron structural environment (31), are nearly identical for complexes **3** and **4** ($\Delta E_{\text{Q}} = 1.94$ and 2.02 mms^{−1}, respectively), whereas that of **2** varies significantly ($\Delta E_{\text{Q}} = 1.27$ mms^{−1}) in a manner consistent with the solid-state structural data for the series.

With respect to the bonding interactions within the BF ligand, the IR spectrum of complex **2** shows a moderately intense band centered at 1407 cm^{−1} assignable to the ν_{BF} stretch (32). This band is higher in energy than that of free BF ($\nu_{\text{BF}} = 1374$ cm^{−1}) (33) and the matrix-produced terminal fluoroborylene complexes Zr(BF)F₂ and Hf(BF)F₂ ($\nu_{\text{BF}} = 1373$ and 1378 cm^{−1}, respectively) (21). However, it agrees well with those calculated with density functional theory methods for Fe(BF)(CO)₄ ($\nu_{\text{BF}} = 1465$ cm^{−1}) (19) and the model complex Fe(BF)(CO)₂(CNAr^{Ph2})₂ (**2m**, $\nu_{\text{BF}} = 1416$ cm^{−1}; Ar^{Ph2}, 2,6-(C₆H₅)₂C₆H₃), as well as that for the titanium terminal fluoroborylene species Ti(BF)F₂ ($\nu_{\text{BF}} = 1404$ cm^{−1}) observed under matrix conditions (21). Accordingly, the low-energy nature of these experimental and calculated ν_{BF} bands provides strong indication that B–F multiple bonding is not significant in terminal fluoroborylene complexes.

Density functional theory calculations on model **2m** support this electronic structure description.

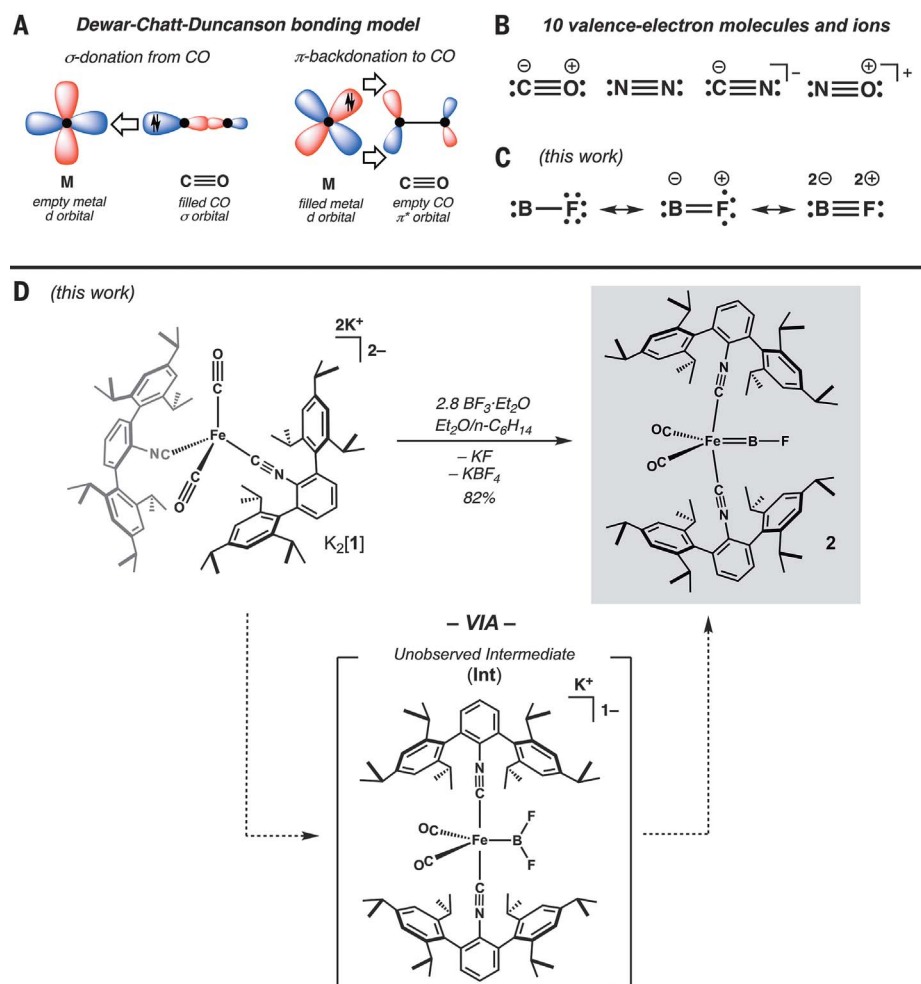


Fig. 1. End-on coordination chemistry of diatomic π -acceptor ligands. (A) Schematic representation of the Dewar-Chatt-Duncanson bonding model for terminal coordination of CO. (B) Well-known 10 valence-electron molecules and ions that function as terminal ligands to transition metals, with formal charges of each atom denoted. (C) Canonical resonance forms of 10 valence-electron BF. (D) Schematic representation of the synthetic route to the iron fluoroborylene complex **2**, including the proposed iron difluoroboryl intermediate **Int**.

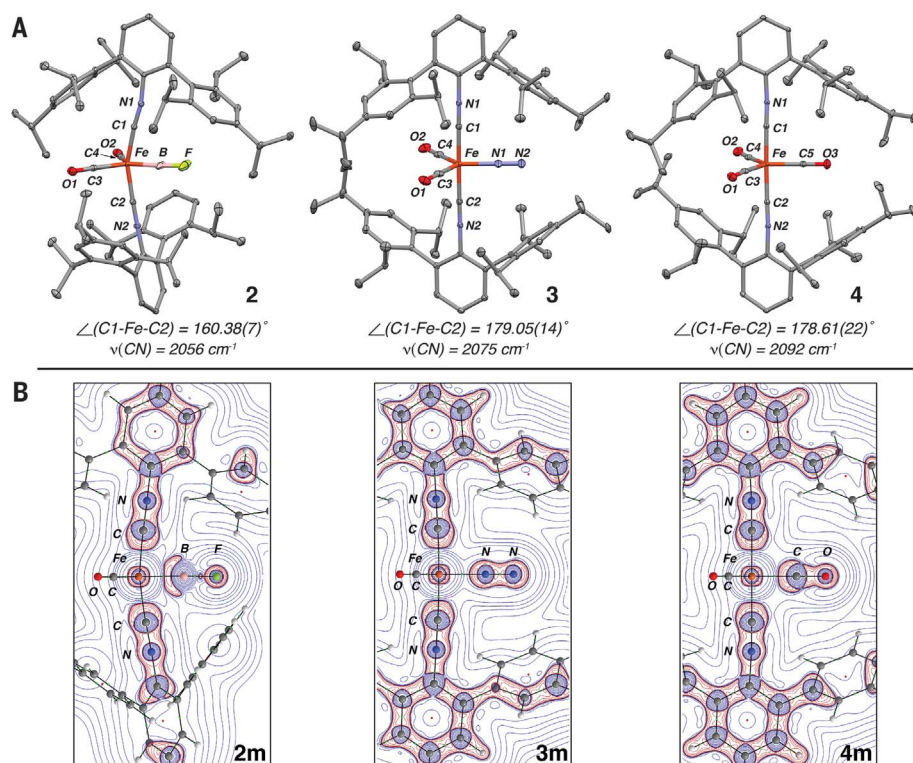


Fig. 2. Crystallographic characterization and electron-density topology calculations of isoelectronic terminal BF, N₂, and CO iron complexes. (A) X-ray crystal structures of the iron fluoroborylene complex **2** and the terminal N₂ and CO complexes **3** and **4**, respectively, along with metrical data for the axial C_{iso}–Fe–C_{iso} angles and IR spectroscopic data for the asymmetric ν_{CN} stretch of each complex. Hydrogen atoms from all structures and one *iso*-propyl group from **2** have been omitted for clarity. Iso, isocyanide. (B) Contour plots of the Laplacian of the electron-density topology (∇²ρ) in the plane containing the iron atom; isocyanide ligands; and BF, N₂, and CO ligand for complexes **2**, **3**, and **4**, respectively. Areas of charge depletion are depicted with blue curves, and areas of charge concentration are depicted with red curves. Bond and ring critical points are denoted with green and red spheres, respectively.

Analysis of the molecular orbitals calculated for **2m** reveal that the ostensible π-bonding orbitals between the fluorine and boron atoms in the molecular *y* and *z* directions (fig. S21) are exceedingly low-lying (HOMO-63 and HOMO-64) and possess predominantly fluorine p-orbital character. As such, these components of the electronic structure of **2m** are best described as fluorine p-orbital lone pairs, rather than B–F π-bonding interactions, and indicate a nominal single bond between the B and F atoms. Natural bond orbital (NBO) analysis also indicates the presence of a B–F single bond in **2m**, yielding a Wiberg bond index of 0.8646 (34). Electron density topology calculations (35) on **2m**, and the model complexes Fe(N₂)(CO)₂(CNAr^{Ph2})₂ (**3m**) and Fe(CO)₃(CNAr^{Ph2})₂ (**4m**), most clearly illustrate the electronic differences between coordinated BF, N₂, and CO ligands. A contour plot of the Laplacian of the electron density (∇²ρ) (Fig. 2B) for **2m** shows a significant depletion of electron density at the BF bond critical point, which is reflective of a highly polarized bonding interaction (35). By contrast, the Laplacian contour plots for the N₂ and CO complexes **3m** and **4m** (Fig. 2B) reveal far greater concentrations of electron density in the regions between N–N

and C–O atoms, respectively, with **3m** displaying a highly symmetric electron-density distribution fully consistent with the presence of nonpolarized, multiple-bonding character (35). Accordingly, although BF is isoelectronic to the 10-electron diatomics CO and N₂, it lacks multiple bonding character between the boron and fluorine atoms and therefore does not possess a similar electronic structure to these ligands when complexed to a transition metal. Moreover, the totality of spectroscopic and computational results suggest that the short B–F bond distance observed for complex **2** manifests simply from a high degree of sp-hybridization of the two-coordinate boron atom, in which the diminished radial extension of the boron 2s orbital relative to its 2p orbitals results in a short BF bond (36).

The molecular design principles and synthetic strategy presented here outline a blueprint for the formation and stabilization of terminal BF ligands on transition metals. Given the particular electronic characteristics of terminally coordinated BF, it is anticipated that this diatomic ligand can be exploited in a general fashion to modulate the physical and chemical properties of transition-metal complexes for specific applications.

REFERENCES AND NOTES

- M. P. Schutzenberger, *Ann. Chim. Phys.* **15**, 100–106 (1868).
- L. Mond, C. Langer, F. Quincke, *J. Chem. Soc. Trans.* **57**, 749–753 (1890).
- M. Elian, R. Hoffmann, *Inorg. Chem.* **14**, 1058–1076 (1975).
- W. A. Herrmann, *J. Organomet. Chem.* **383**, 21–44 (1990).
- M. J. S. Dewar, *Bull. Soc. Chim. Fr.* **18**, C79 (1951).
- J. Chatt, L. A. Duncanson, *J. Chem. Soc.* 2939–2947 (1953).
- F. A. Cotton, C. S. Kraihanzel, *J. Am. Chem. Soc.* **84**, 4432–4438 (1962).
- A. W. Ehlers, S. Dapprich, S. F. Vyboishchikov, G. Frenking, *Organometallics* **15**, 105–117 (1996).
- H. Werner, *Angew. Chem. Int. Ed. Engl.* **29**, 1077–1089 (1990).
- R. K. Nesbet, *J. Chem. Phys.* **40**, 3619–3633 (1964).
- P. L. Timms, *J. Am. Chem. Soc.* **89**, 1629–1632 (1967).
- P. L. Timms, *J. Am. Chem. Soc.* **90**, 4585–4589 (1968).
- F. J. Lovas, D. R. Johnson, *J. Chem. Phys.* **55**, 41–44 (1971).
- P. L. Timms, *Acc. Chem. Res.* **6**, 118–123 (1973).
- C. Esterhuysen, G. Frenking, *Theor. Chem. Acc.* **111**, 381–389 (2004).
- A. W. Ehlers, E. J. Baerends, F. M. Bickelhaupt, U. Radius, *Chemistry* **4**, 210–221 (1998).
- U. Radius, F. M. Bickelhaupt, A. W. Ehlers, N. Goldberg, R. Hoffmann, *Inorg. Chem.* **37**, 1080–1090 (1998).
- F. M. Bickelhaupt, U. Radius, A. W. Ehlers, R. Hoffmann, E. Jan Baerends, *New J. Chem.* **22**, 1–3 (1998).
- L. Xu, Q. S. Li, Y. Xie, R. B. King, H. F. Schaefer 3rd, *Inorg. Chem.* **49**, 1046–1055 (2010).
- D. Vidovic, S. Aldridge, *Angew. Chem. Int. Ed.* **48**, 3669–3672 (2009).
- X. Wang, B. O. Roos, L. Andrews, *Angew. Chem. Int. Ed.* **49**, 157–160 (2010).
- X. Wang, B. O. Roos, L. Andrews, *Chem. Commun.* **46**, 1646–1648 (2010).
- H. Braunschweig, K. Kraft, T. Kupfer, K. Radacki, F. Seeler, *Angew. Chem. Int. Ed.* **47**, 4931–4933 (2008).
- H. Braunschweig, R. D. Dewhurst, *Angew. Chem. Int. Ed.* **49**, 3412–3414 (2010).
- A. E. Carpenter *et al.*, *Inorg. Chem.* **54**, 2936–2944 (2015).
- J. P. Collman, *Acc. Chem. Res.* **8**, 342–347 (1975).
- H. Braunschweig, R. D. Dewhurst, V. H. Gessner, *Chem. Soc. Rev.* **42**, 3197–3208 (2013).
- H. Braunschweig, K. Radacki, A. Schneider, *Science* **328**, 345–347 (2010).
- L. Mueller, *J. Am. Chem. Soc.* **101**, 4481–4484 (1979).
- A. Bax, S. Subramanian, *J. Magn. Reson.* **67**, 565–569 (1986).
- P. Gütlich, E. Bill, A. X. Trautwein, *Mössbauer spectroscopy and transition metal chemistry: Fundamentals and applications*. Springer: Berlin (2011).
- The IR stretch from the ¹⁰B isotopologue, expected at ~1451 cm⁻¹ from a reduced mass calculation, is masked by a band of moderate intensity at 1456 cm⁻¹ stemming from an aromatic C–C stretch of the meta-terphenyl ligands. Additional details are in the supplementary materials.
- P. Hassanzadeh, L. Andrews, *J. Phys. Chem.* **97**, 4910–4915 (1993).
- J. P. Foster, F. Weinhold, *J. Am. Chem. Soc.* **102**, 7211–7218 (1980).
- R. F. W. Bader, *Chem. Rev.* **91**, 893–928 (1991).
- R. J. Gillespie, E. A. Robinson, *J. Comput. Chem.* **28**, 87–97 (2007).

ACKNOWLEDGMENTS

We thank C. Cummins, G. Debelouchina, and B. Barnett for helpful discussions. **Funding:** This work was supported by the U.S. National Science Foundation through grants CHE-1802646 (to J.S.F) and CHE-1454370 (to M.L.N). **Author contributions:** M.J.D. carried out the synthetic work, analytical characterization, and computational studies. J.D.S. and M.L.N. performed the Mössbauer spectroscopy studies. A.M.M. devised and performed the 2D NMR experiments. M.J.D., C.E.M., and A.L.R. carried out the crystallographic studies. J.S.F. assisted with data analysis and directed the research. M.J.D. and J.S.F. wrote the manuscript, with input from all authors.

Competing interests: Authors declare no competing interests. **Data and materials availability:** X-ray data are available free of charge from the Cambridge Crystallographic Data Centre under references CCDC-1887069 (**2**), CCDC-1887070 (**3**), CCDC-1887071 (**4**), and CCDC-1887072 (K₂**1**). Additional spectroscopic, crystallographic, and computational data are included in the supplementary materials.

SUPPLEMENTARY MATERIALS

www.sciencemag.org/content/363/6432/1203/suppl/DC1
Materials and Methods
Supplementary Text
Figs. S1 to S30
Tables S1 to S10
References (37–70)

9 January 2019; accepted 19 February 2019
10.1126/science.aaw6102

Terminal coordination of diatomic boron monofluoride to iron

Myles J. Drance, Jeffrey D. Sears, Anthony M. Mrse, Curtis E. Moore, Arnold L. Rheingold, Michael L. Neidig and Joshua S. Figueroa

Science **363** (6432), 1203-1205.
DOI: 10.1126/science.aaw6102

Iron's new Best Friend

Carbon monoxide (CO) is one of the most widely studied ligands in the chemistry of transition metals. One of its distinguishing features is a two-way bonding motif, in which CO donates electrons to the metal while the metal simultaneously engages in "back bonding" in the other direction. Theory has suggested that the isoelectronic boron fluoride diatomic, BF, would be even more effective at both types of bonding. However, it has been challenging to prepare the requisite compounds for comparison. Drance *et al.* now report synthesis of a terminal iron-BF complex, with donor and acceptor characteristics that compare favorably to analogous CO and N₂ complexes.

Science, this issue p. 1203

ARTICLE TOOLS

<http://science.sciencemag.org/content/363/6432/1203>

SUPPLEMENTARY MATERIALS

<http://science.sciencemag.org/content/suppl/2019/03/13/363.6432.1203.DC1>

REFERENCES

This article cites 67 articles, 1 of which you can access for free
<http://science.sciencemag.org/content/363/6432/1203#BIBL>

PERMISSIONS

<http://www.sciencemag.org/help/reprints-and-permissions>

Use of this article is subject to the [Terms of Service](#)